This paper describes objective technical results and analysis. Any subjective views or opinions that might be expressed in the paper do not necessarily represent the views of the U.S. Department of Energy or the United States Government.

ASTFE
American Society of Thermal and Fluids Engineers

4th Thermal and Fluids Engineering Conference (TFEC)
Las Vegas, NV, USA

SAND2018-11414C

TFEC-2019-xxxxx

COMPOSITE MATERIAL COMBUSTION MODELING USING THERMALLY INTERACTING, CHEMICALLY REACTIVE LAGRANGIAN PARTICLES

Flint Pierce[1*], Alexander L. Brown[1], Tyler Voskuilen[1], Heeseok Koo[1,2]

[1]Sandia National Laboratories, Albuquerque, NM 87105, USA
[2]Rolls Royce Indianapolis, IN, USA

ABSTRACT

Heterogeneous material combustion presents several difficulties to computational simulation. These difficulties correlate with the complex phenomena observed during a fire containing laminated epoxy carbon fiber-filled composites. Among these are non-trivial thermal and gas transport within/between composite layers and the surrounding gas phase as well as chemical degradation of composite materials, including smoldering which can persist for periods of several hours. In this paper, we describe a new approach to modeling burning and thermal transport in carbon fiber-filled epoxy laminates via an ensemble of thermally interacting, chemically reacting Lagrangian particles. These particles are arranged in conformations consistent with individual layered composite laminate pieces. The particle ensemble represents the topology of a pile of composite rubble where thermal conduction occurs within and between layers, a function of the particle positions, sizes, and constituent material properties. Particle reactions proceed according to selected chemical mechanisms resulting in enthalpy, mass, and momentum transfer between the particle and gas phases as well as thermal transport between neighboring particles. Here we present the results of a small set of example scenarios and discuss the efficacy of this approach. We briefly discuss coupling of this capability to a Volume of Fluid approach for mixed phase (liquid, gas, solid) combustion for scenarios with both liquid and solid combustibles.

KEY WORDS: Combustion, Fuego, Particles, Composite, Lagrangian, Chemistry

1. INTRODUCTION

Laminated composite materials, due to their superior strength to weight ratios, are now commonly used in a variety of aerospace applications. These materials are regularly fabricated in layered conformations composed of carbon fiber-filled epoxy bound with various binders. They can experience novel thermal and chemical behaviour in diverse accident scenarios due to their complex structure and material constituents. Particularly challenging is the fact that the epoxy can respond to high heat fluxes and/or temperature by reacting to evolve gas species which may themselves be combustible. Additionally, embedded carbon fibers and char from combusted epoxy can continue to smolder through slow oxidative processes for hours. The evolution of the burning process is highly dependent on the geometric configuration of rubble as well as environmental conditions. This has been observed through a series of composite fire tests performed over the last several years at SNL [1-6]. SNL is not alone in its interest in combusting laminated composite materials, and a number of other researchers have investigated the process [7-17].

Most recently, a concern has been raised for scenarios in which an aerial vehicle accident results in composite rubble partially or wholly immersed in residual liquid fuel. In such cases, at least three distinct material phases are present: a gas or fluid phase of air and evolving/combusting gases, a liquid fuel phase, and a solid phase composed of composite rubble material, though other solid phase materials may also be present.

*Corresponding Author: fpierce@sandia.gov

Sandia National Laboratories is a multimission laboratory managed and operated by National Technology & Engineering Solutions of Sandia, LLC, a wholly owned subsidiary of Honeywell International Inc., for the U.S. Department of Energy's National Nuclear Security Administration under contract DE-NA0003525.

To facilitate investigation of composite combustion, researchers at SNL have begun using computational models of composite material fires, utilizing experimental test results to validate these models. SNL Sierra developers have implemented these models within two primary codes, Sierra low-Mach module Fuego which is the primary CFD tool used for low-Mach laminar or turbulent reacting flow cases (combustion, etc.) and Sierra multi-physics module Aria, the principle code used for thermal transport, organic material decomposition, energetic materials, and a variety of other physics applications. Specific composite material combustion models vary in thermal and chemical description, and SNL has tested a set of variants, including a continuum model of the burning material within Aria loosely coupled to a CFD fluid region in Fuego. A second model utilizes a simplified 1D composite fire boundary condition completely within Fuego [18, 19]. Uncertainty quantification and verification/validation have been integrated into the evaluation of these models throughout this process via a suite of computational/experimental studies [1-3, 18, 20-22].

Each of the approaches described above has advantages, but both lack the ability to readily simulate the scenario of more recent interest, a geometrically complex burning pile of composite rubble in a pool of liquid fuel. In response to this need, we have designed and implemented a novel reacting composite material approach utilizing Fuego's native Lagrangian particle capability. In this scheme, composite bars are modelled as layers of chemically reacting, thermally interacting particles, coupled to the background fluid (gas species) through mass, momentum, energy, and species transport equations. This approach enables a full three-dimensional description of composite material combustion including chemical reactions and thermal and gas transport. Despite this, solid combustion remains an incredibly complex process, especially for materials like laminated composites. This new capability is meant to aid in modelling laminated composite combustion, though the complexities of thermal and fluid transport as well as the complex chemistry involved remain significant challenges.

We present here the details of this model as well as the results from a selection of demonstration scenarios. While these examples are intended to demonstrate the capability, they are not parameterized to a particular composite material or fire scenario. In each case, a sufficient number of Lagrangian particles has been used to highlight the coupled processes of inter-particle thermal conduction and particle-level chemistry. In a realistic scenario, one would use a much larger number of Lagrangian particles as well as empirically determined chemical mechanisms and thermal properties.

2. COMPUTATIONAL MODEL

2.1 CFD and thermal radiation transport

Sierra low-Mach module Fuego provides a CFD capability for modelling laminar or turbulent reacting flows. It has been demonstrated for gas phase combustion at a variety of length and time scales, and has been applied over a wide range of low-Mach CFD applications [19, 22-25].

A Lagrangian particle capability is also available in Fuego which includes particles of a variety of types (tracer, heated, inertial, wildfire, evaporating, etc.) for transport within the fluid domain. This capability has enabled simulation of wildfire spread, evaporating particles, aluminium propellant combustion, contaminant transport, etc. Fuego utilizes a loose coupling mechanism for fluid and particle regions where execution of specific physics algorithms and transfer of relevant source terms between the Eulerian fluid region and Lagrangian particle regions is managed. Such transfers include species, mass, energy, and momentum terms.

Fuego also supports radiative heat transport through legacy Sierra radiation heat transport module Syrinx as well as more recently through RAMSES Scefire and open source low-Mach code Nalu through an MPMD (multiple program multiple data) approach. The participating media radiative transport provided by these codes uses the discrete ordinates method (DOM) of angular discretization. Radiative transport includes both fluid and particle terms.

2.2 Reacting, thermally interacting particles

Recently, a general chemistry capability has been adopted in Fuego to facilitate solid and solid/fluid phase reaction models at the particle level. We will not exhaustively describe this chemistry mechanism in detail here, only to say that Arrhenius type reaction forms can be specified which involve both particle and fluid species.

Historically, Fuego Lagrangian particles have not interacted with each other in an explicit manner, though they have indirectly interacted through coupling to the fluid. Over the last few years, a capability for handling particle momentum/force interactions has been implemented and demonstrated for droplet breakup in a crosswind [19,26] using a modified Lennard-Jones type force field. For the current study, we have enhanced this capability by implementing a mechanism to handle thermal interactions between neighboring particle pairs.

Fuego Lagrangian particles are idealized as spherical particles with a single length scale, the diameter. Particle position and velocities within the mesh are tracked. For chemically reactive particles, we also monitor the particle temperature and constituent material components in terms of material mass fractions. In regards to the thermal conduction between particles, we idealize this process as binary; that is, heat is seen to be transferred from pairs of particles in near contact as shown in Figure 1. From a knowledge of particle material properties and temperatures, one can calculate a pairwise thermal conduction in the following way:

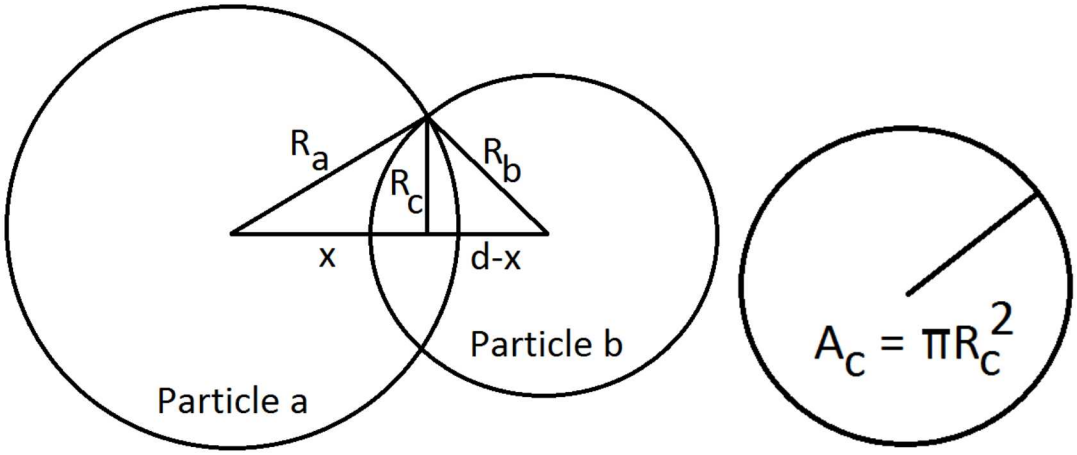

Fig. 1 Particles a, b of radii R_a, R_b, with center-to-center separation d, in thermal contact at a circle with radius R_c and contact area A_c.

In Figure 1, two particles (a, b) of radii R_a and R_b , respectively, are at a center-to-center separation d in thermal contact along a circular region with overlap radius R_c and area A_c. This contact circular area is located a distance x from the center of particle a. From simple geometric arguments we find:

$$x = \frac{d^2 + {R_a}^2 - {R_b}^2}{2d} \tag{1}$$

and:

$${R_c}^2 = {R_a}^2 - x^2 \, , A_c = \pi {R_c}^2 \tag{2}$$

The thermal conduction rate between these particles can be described as:

$$P_{a,b} = \frac{A_c(T_a - T_b)}{\frac{d-x}{k_b} + \frac{x}{k_a}} \tag{3}$$

Where k_a, k_b are the thermal conductivities and T_a,T_b the temperatures of particles a and b, respectively.

Note that in the limit $R_a \ll R_b$, we have $d \approx R_b$, $x \approx 0$, and:

$$P_{a,b} \approx \frac{k_b A_c(T_a - T_b)}{R_b} \tag{4}$$

indicating that thermal conduction is dominated by particle b (and material b). In the other limit, that is, $R_a \gg R_b$, we have $d \approx R_a$, $x \approx R_a$, and:

$$P_{a,b} \approx \frac{k_a A_c(T_a - T_b)}{R_a} \tag{5}$$

so that thermal conduction between the particle pair is principally through material a.

Fuego solves the equations of motion (trajectories) for reacting, thermally interacting Lagrangian particles through a standard ODE solver in a monolithic sense. Several standard ODE solvers are available including standard CVODE, LSODE, and a variety of Runge-Kutta methods. Since particle equations of motion are solved one particle at a time, a user must make certain that a sufficiently small timestep is used to resolve the thermal conduction between particles. The position, velocity, temperature, and species constituents are all solved simultaneously through the ODE solver. Particle equations of motion can be solved at a finer timescale than the CFD fluid equations, which can be important for particles experience fast chemical reactions as is often observed in Arrhenius style reaction mechanisms.

For the current application, that of a rubble pile of composite plates resulting from some accident, we have chosen to represent the pile as a geometrically arranged collection of individual plates or *bars*. These bars are composed of an ensemble of composite particles in close thermal contact residing in *layers*. Heat conduction is not allowed between different bars, and it is reduced by a constant factor through neighboring layers within the same bar. Bars are arranged in a random orientation with respect to each other, as one might expect from an accident scenario.

Figure 2 below shows an example particle configuration composed of two bars, each with three layers.

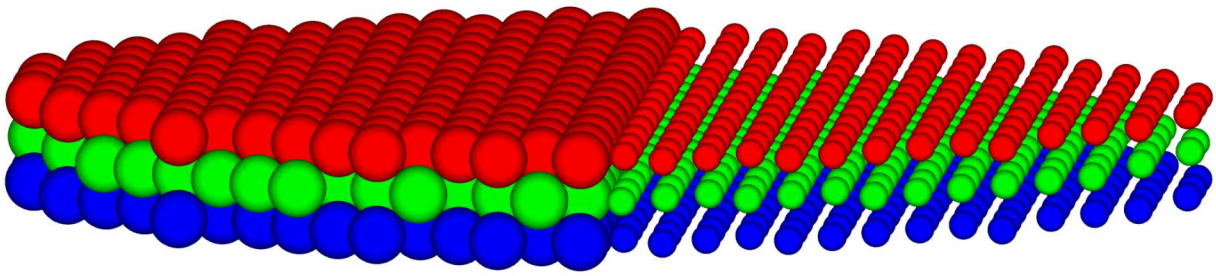

Fig. 2 Composite particle example with particles arranged in two neighboring *bars*, each composed of 3 *layers*. Here, size indicates bar in which particle is found, with layer indicated by color. Particles in same bar and layer have full thermal conduction. Those within same bar but neighboring layers have reduced conduction. Particles in different bars have no thermal conduction.

Analysts initialize these particle simulations by specifying particle location, size, temperature, bar and layer identification, chemical mechanisms, material properties, and fluid volumetric and boundary conditions. Particles are initialized with mass fraction based composition with specific particle materials for which various properties are defined, including density, specific heat, thermal conductivity, absorptivity, surface tension, film Prandtl number, etc. Composite particles are fixed in space for these examples.

3. SIMPLE EXAMPLE

For demonstration purposes, we have created a simple configuration of 34 particles in thermal contact and without any active chemical reaction mechanisms. This case demonstrates the thermal conduction as a function of *bars* and *layers*. The initial particle configuration including position, bar and layer identification, is shown in Figure 3 (left). Each sphere corresponds to a single particle, and the size of the sphere indicates the *bar* in which the particle lies (1 to 3). Particles lying within bars 2 and 3 are shown connected by lines for clarity. The color of each particle indicates the "layer" number. Thus, the entire lower-left branch, central particle, and the first 6 particles of the lower-right and upper branch all lie within the same bar and layer (1,1). Initial temperatures for each particle are as labelled beside each particle (300K and 800K). The upper branch contains particles residing in two other bars (2 and 3) in the same orientation as bar 1, and close enough for thermal contact. As stated above, no direct particle heat conduction is allowed between particles in different bars. The lower right branch contains 5 particles that lie in bar 1 but increasing in layer number (2 to 6). For these particles, direct heat conduction can occur but at a reduced value to that within the same layer. For this example, the thermal layer reduction factor is 0.2.

Thermal contact is maintained between the particles by using a linear expansion factor for the diameter of 1.2. This is necessary for all such thermal contact where particles are normally placed no closer than 1 diameter apart, which would make their unmodified contact area be identically zero (see Eqs. 1 and 2). As a consequence of this expansion factor, there is a slight difference between aerodynamic (drag) and thermal diameters for particles.

All particles used in this idealized case are composed of a single material. Particle and material properties are listed in Table 1.

Table 1 Particle and particle material properties used in demonstration example 1

Particle Property	Symbol	Value	Units
diameter	d	0.02	m
density	ρ	1779	kg/m^3
specific heat	C_p	866	J/kg·K
absorptivity	α	1.0	
viscosity	ν	100	Pa·s
thermal conductivity	k	50.0	W/m·K
surface tension	σ	1000.0	N/m
film Prandtl number	Pr_{film}	1.0	

The fluid domain is a 50cm x 100cm x 50cm region initialized with an atmosphere composed of 23.3% O_2 and 76.7% N_2 at T_i = 300K, lower and side walls at T_{wall} = 300K and upper open boundary also at T_{open} = 300K.

A timestep of 0.3s is used over the duration of the simulation, which extends to 500s.

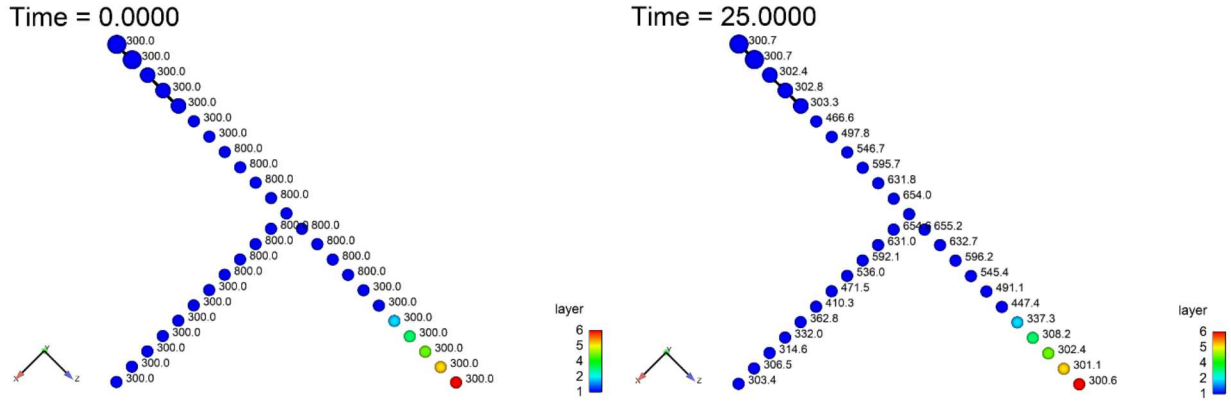

Fig. 3 Simple interparticle conduction example. Left – initial particle temperatures shown. Right – particle temperatures after t = 25s. Bar # represented by size, Layer # by color, T as indicated. For clarity, particles within bars 2 and 3 are shown connected by lines.

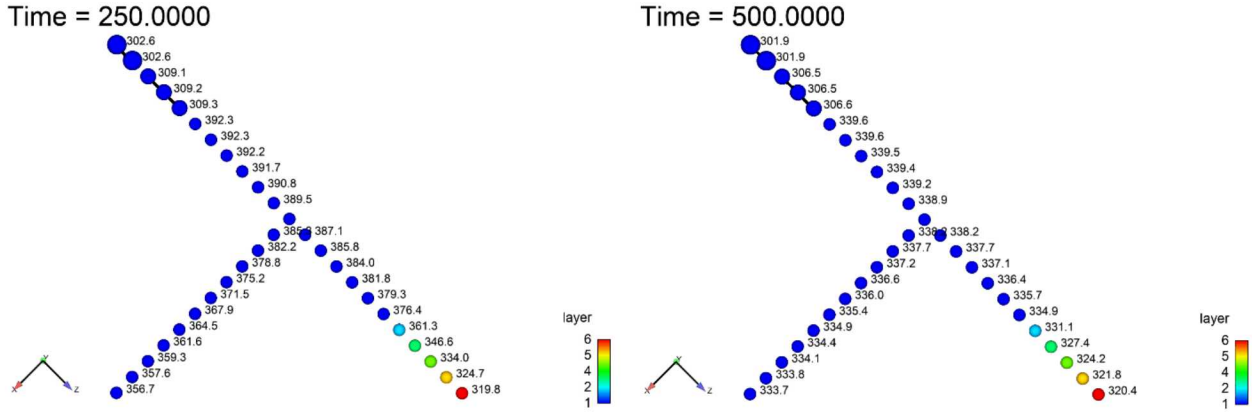

Fig. 4 Simple interparticle conduction example. Left – particle temperatures shown at t = 250s. Right – particle temperatures after t = 500s. Bar # represented by size, Layer # by color, T as indicated. For clarity, particles within bars 2 and 3 are shown connected by lines.

Figures 3 and 4 demonstrate several important aspects of interparticle thermal conduction using this model. First, by comparing conduction through the three branches, one can readily see that conduction through the lower-left branch where all particles are within the same bar and layer proceeds unimpeded and faster than either of the other two branches where this is not the case. Second, conduction does proceed, albeit at a slower rate, through the lower right branch in which particles at the end of the branch lie in different layers. Finally, inter-particle conduction in the upper branch is eliminated across bar boundaries. Particles in bars 1 and 2 do heat up slightly due to indirect thermal coupling via heating of the background fluid by nearby particles. As a result, we see particles in bar 2 at around 307K at late times, and particles in bar 3 at approximately 302K at late times, while particles in bar 1 on this branch are at nearly 339K.

These results are consistent with the thermal transport mechanism we have described in the model section. During implementation of the thermal conduction model, a number of simpler verification tests were performed to verify the correctness of the interparticle thermal transport mechanism, but for space we omit those results here.

4. SINGLE LAYER OF REACTING PARTICLES

In this next example, we demonstrate the use of a particle chemical reaction mechanism in tandem with interparticle thermal conductivity. For this case, a single bar/layer composed of 9801 monodisperse particles of

size d = 1cm (square 99 particles on a side) are placed horizontally at a position 10cm below the vertical center of a 1m x 1m x 1m cubic domain. The particles are all initialized at $T_{p,i}$ = 300K. The volume of the cube is initialized with a fluid temperature of $T_{f,i}$ = 800K, with gas mass fractions of $Y(O_2)$ = 0.2314, $Y(N_2)$ = 0.7686. The lower boundary is a fluid inflow at T_{inflow} = 800K and identical gas mass fractions with a z-velocity (upward) of 1.0 m/s. The vertical sides of the domain are isothermal walls held at a constant T_{wall} = 800K. The top surface is an open boundary with a fixed temperature of 800K and the same gas mass fractions as already stated which allows outflow of evolved gases. Figure 5 shows a snapshot at t = 16s for this configuration. Particles are illustrated as a horizontal layer of spheres, which at t = 16s are in the approximate range T_p = 550K - 650K. Three cut planes are also shown at y = 0, and z = ±0.3m. Arrows indicate and are colored by fluid velocities.

The chemical mechanism for the particles is defined as an Arrhenius form, converting particle species A to particle species B and gas phase CH_4 through the reaction mechanism:

$$A \rightarrow 0.5B + 0.5CH_4$$

The rate follows an Arrhenius form with a rate ω (moles/m^{3}s) of:

$$\omega = f \exp\left(-\frac{\mathrm{E}_a}{\mathrm{RT}}\right)$$

Where the reaction prefactor f = $3.33 \cdot 10^{15}$ (moles/m^{3}s), activation energy E_a = $2.2614 \cdot 10^5$ J/mol, and R the ideal gas constant 8.314 J/mol·K

Particle material A is identical to that used in the previous example, and particle material B is similar to A with the following changes: C_p = 936.4 J/kg·K , σ = 0 N/m , and Pr_{film} = 0.99:

Figure 6, at 5 later times, and Figure 7, over the active time range for the simulation, show the increase in T_f as evolved CH_4 begins to burn. Here we use the Eddy Dissipation Concept (EDC) combustion model that is standard in Fuego. After the start of gas phase combustion, particles heat at an increasing rate, eventually overshooting the wall and initial volumetric temperature of 800K, reaching a peak $T_p \approx$ 1050K. During the fastest reaction period, where the most CH_4 is being evolved from the particles, between 18 and 22s as seen in Figure 8, fluid velocities also peak. Once the period of CH_4 evolution subsides, gas phase and particle temperatures fall. The hot gas exits the simulation domain rapidly due to the inflow of the T_f = 800K inflow at 1 m/s. The maximum particle temperature falls over an extended period of time due to their relatively large thermal mass.

The above described burning process is consistent with our intuition regarding the burning of organic materials like wood or charcoal. Once the temperature of the material becomes sufficient to activate reaction, and in the presence of sufficient oxygen, the material burns. Combustion of gas phase products increases the heat flux to and consequently the temperature of the burning solid materials. This continues until the combustible gas products begin to subside as a result of elimination of reactants, and the residual solid material cools. This example does not include a slow exothermic oxidative char oxidation reaction which would result in long-term smoldering.

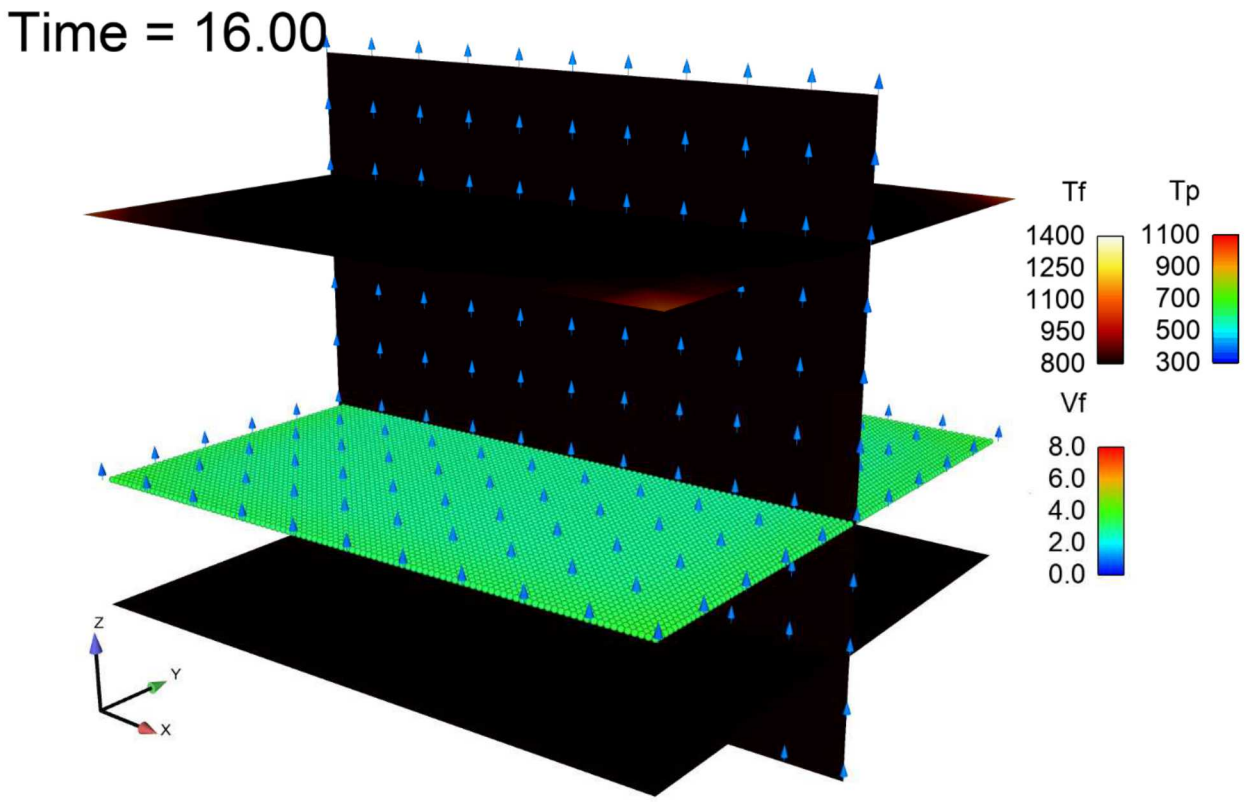

Fig. 5 Reacting thermally-interacting particle case. At t = 16s, particles colored by particle temperature, T_p (K). Vertical and horizontal cut planes colored by the fluid temperature T_f (K). Arrows are sized and colored by fluid velocity V_f (m/s).

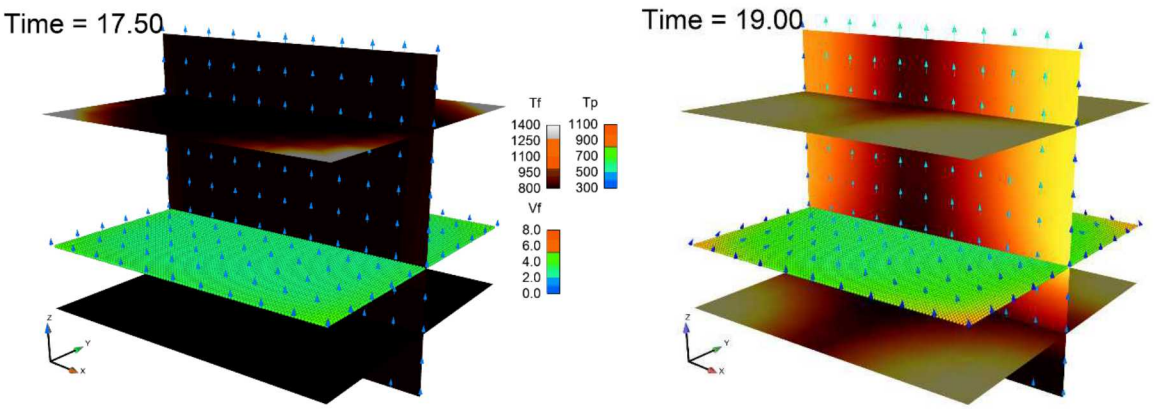

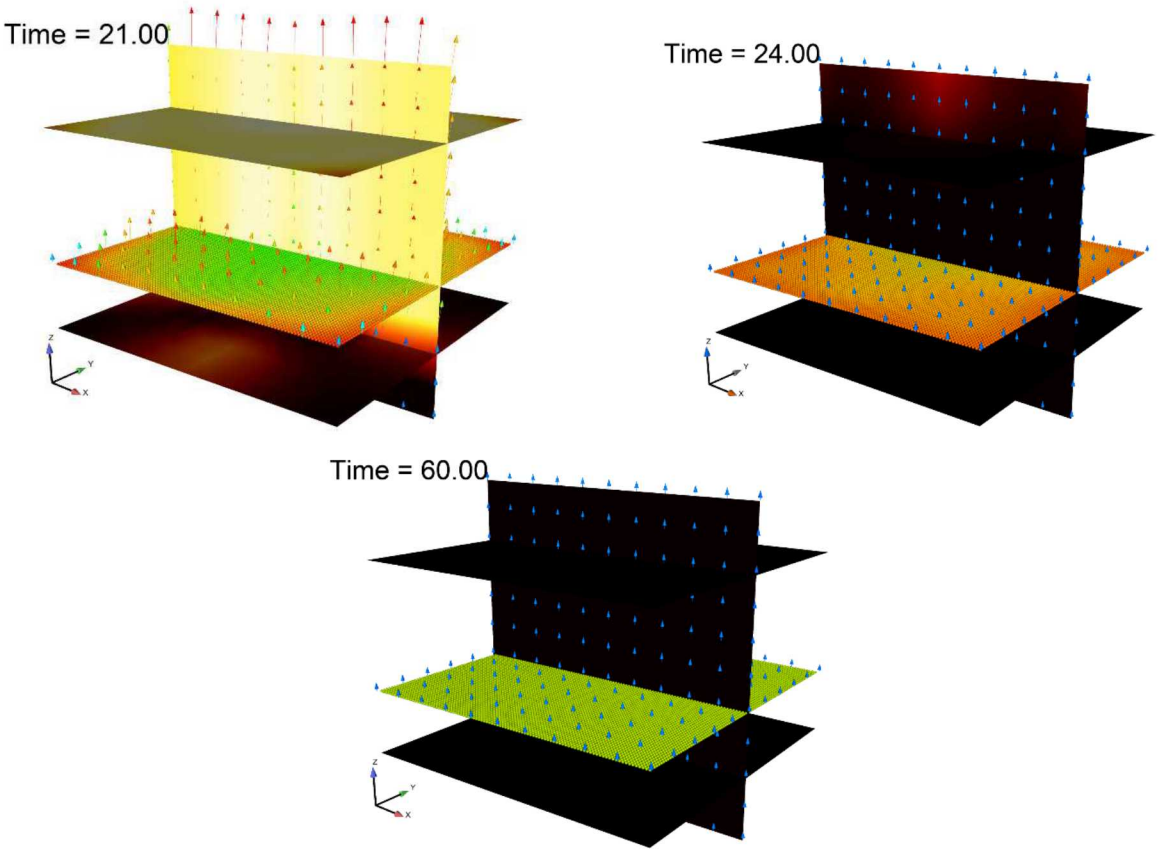

Fig. 6 Reacting, thermally-interacting particle case. Display of particles/fluid as in Fig. 5. At t = 17.5s, fluid starts heating up from combusting particle gases. By 19s, combustion increasing temperature, fluid velocity direction effected. By 21s, high fluid velocities/temperature, particles heating up. By 24s, particle reactions mostly finished, fluid temperatures near initial value. By 60s, particles have cooled to ambient fluid temp.

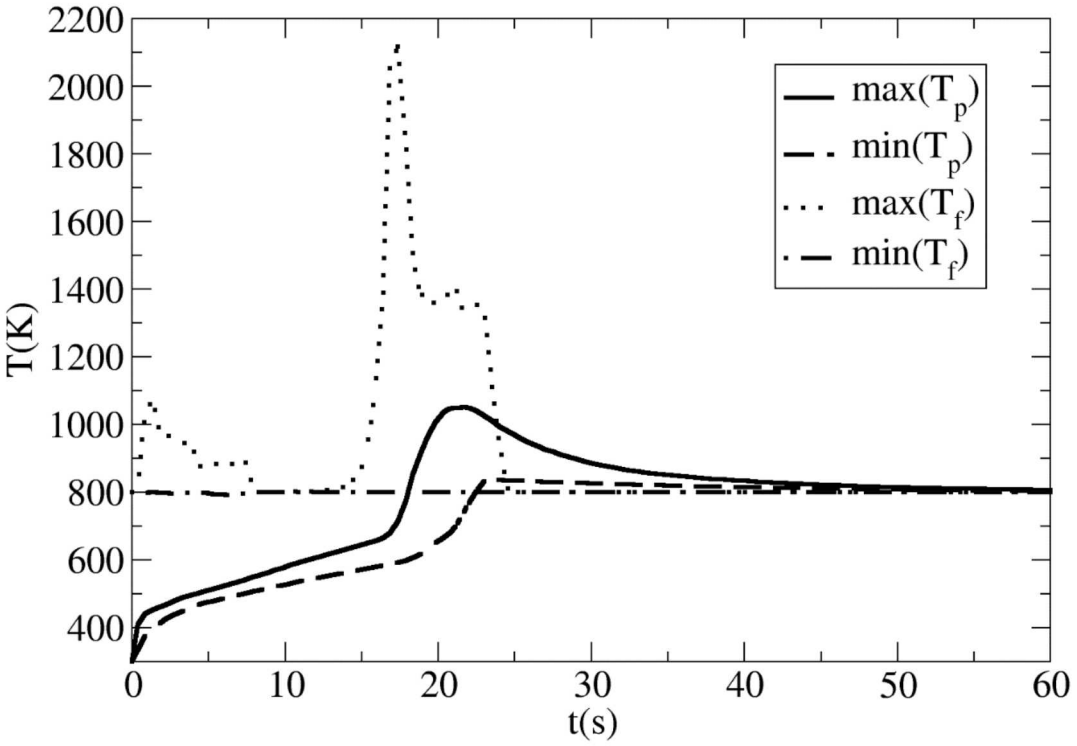

Fig. 7 Reacting, thermally-interacting particle case. Transient maximum and minimum fluid (Tf) and particle temperatures (Tp) shown. As Tp → 650K, particle reaction mechanism evolves combusting gas, causing rapid rise in T_f, further increasing T_p (to about 1050K). Once gas products nearly exhausted (t ~ 21s), T_f rapidly falls, and T_p asymptotically approaches 800K.

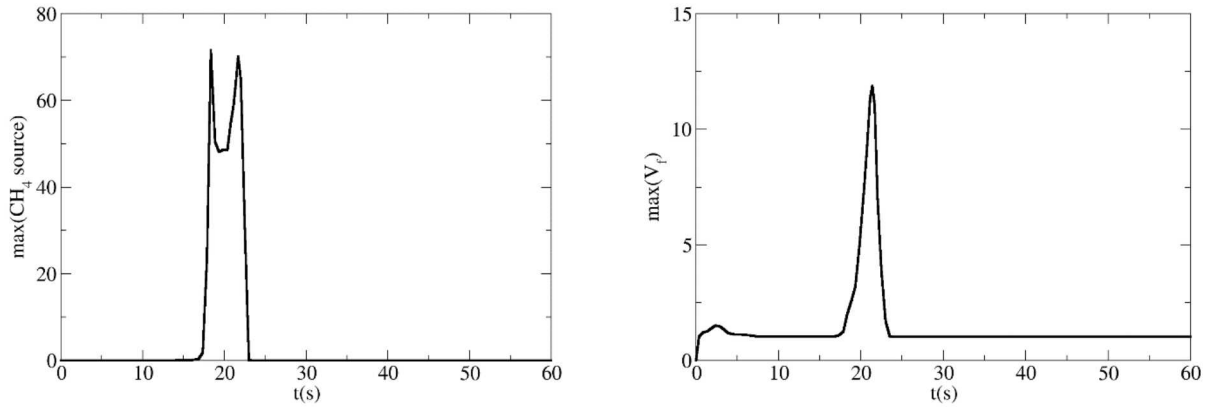

Fig. 8 Maximum fuel source term (CH_4 source) and fluid velocity Vf (m/s)over the course of the simulation.

5. MULTIPLE BARS/LAYERS OF REACTING, THERMALLY-INTERACTING PARTICLES

This final case simulates a randomly oriented rubble pile of composite panels as might arise during an accident scenario. The simulation domain is limited to 0.5m x 1.0m x 0.5m. 50 rectangular bars composed of between 1 and 3 layers of reacting particles (9559 particles in total) is shown in the upper-left frame of Figure 9. Particles are displayed with size and shading corresponding to the layer in which they are placed. For this case, particles are given thermal diameters 1.2 times larger than their aerodynamic diameter to guarantee thermal contact. Thermal conductivity between particles in adjacent layers is reduced by a factor of 0.01, and as before is disallowed between different rectangular bars in contact. Additionally, particle reactions and materials are identical to the previous case. The lower boundary for the simulation domain is an upward 1.0 m/s inflow at T = 1000K, sufficiently high to initiate particle chemical. Vertical sides walls are isothermal at 800K, and the upper surface is an open boundary, also at 800K.

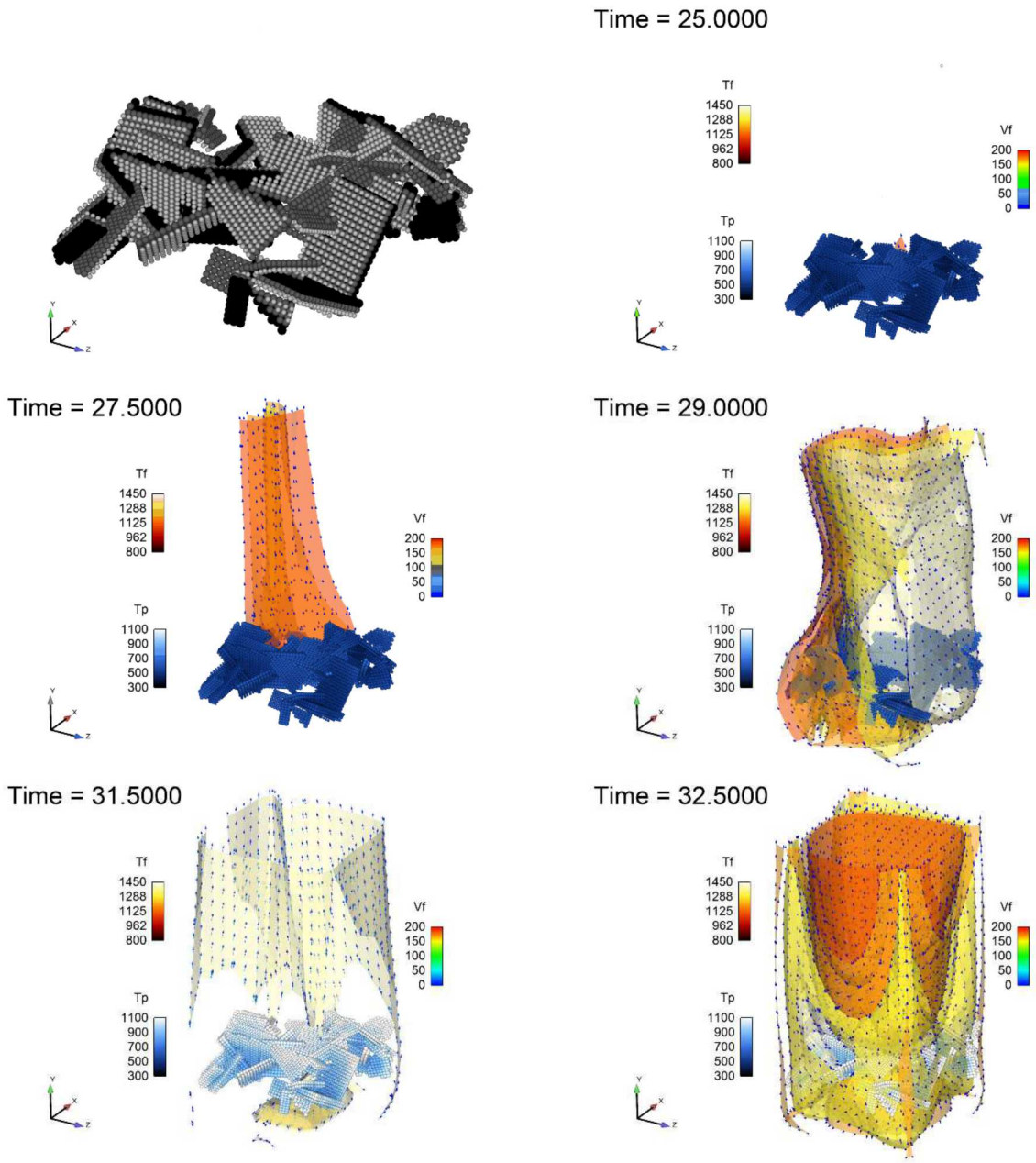

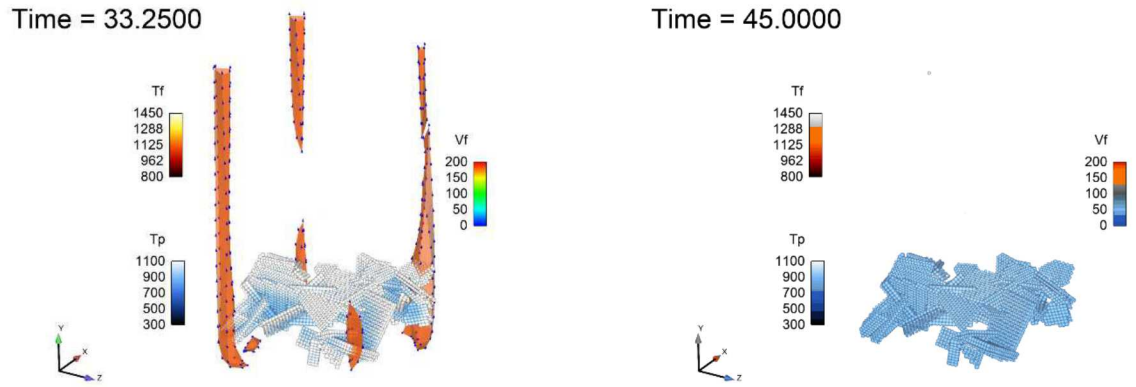

Fig. 9 Multiple bar/layer rubble pile example. (Upper left): initial configuration – size/shading indicates particle layer. (Upper right – Lower Right) At several simulation times, particles shown shaded by temperature (Tp) - dark blue to white with scale set to Tp_{min} (300K) to Tp_{max} (1100K) over full simulation time. Four fluid temperature (Tf) isosurfaces shown (1100K – 1400K), shaded from dark red to yellow. For each isosurface, arrows are shown, colored by fluid velocity (Vf).

Results for this case are displayed in Figure 9. The upper left frame shows the initial particle configuration with sizes and shading representing the layer for each particle. In each of the additional display frames, taken over the course of the simulation, the time is shown with composite particles shaded by particle temperature T_p. A set of fluid temperature (T_f) isosurfaces are also displayed, colored for 4 different values of T_f: 1100K, 1200K, 1300K, and 1400 K. On each T_f isosurface, arrows are shown and colored by fluid velocity.

Here again we observe that heating of particles by the surrounding fluid results in outgassing of combustible gases from the particles followed by gas phase combustion by this fuel species. The evolved heat then drives up the temperature of the particles which further increases the rate of reaction. Eventually, gas phase products are exhausted and particles cool to ambient conditions.

6. CONCLUSIONS AND COUPLING TO LIQUID FUEL

In this work we have outlined a novel Lagrangian particle/Eulerian fluid approach to modeling the physical process of thermal transport and chemical reactivity in composite materials coupled to gas phase combustion. Phenomenologically, the combustion process is consistent with what we know and would expect of burning organic materials, including heat conduction within and between material layers, temperature dependent chemical reactions, evolution and subsequent combustion of gas species from the reacting solid material followed by slow cooling of particles subsequent to pyrolysis.

This capability is the first of two components required for simulation of combined (liquid/solid) fuel environments such as one would observe in an accident scenario involving an aerial vehicle with laminated epoxy carbon fiber-filled components. Other members of our team have implemented a volume of fluid (VOF) method for modeling liquid fuel motion and evaporation, also within Sierra low Mach module Fuego. This model is currently being tested, and we have started coupled VOF/composite particle simulations relevant to the scenarios of interest. The results of these studies will be published in a subsequent SAND report.

ACKNOWLEDGMENT

Sandia National Laboratories is a multimission laboratory managed and operated by National Technology and Engineering Solutions of Sandia, LLC., a wholly owned subsidiary of Honeywell International, Inc., for

the U.S. Department of Energy's National Nuclear Security Administration under contract DE-NA-0003525. This work was funded by the Nuclear Safety Research and Development Program under the Rubble Fire project.

NOMENCLATURE

d	center-center particle separation	(m)	$T_{a,b}$	contacting particle temperatures	(K)
$R_{a,b}$	radii of particle in thermal contact	(m)	$k_{a,b}$	thermal conductivity of particles	(W/m·K)
x	particle to thermal contact circle distance	(m)	A_c	area of thermal contact circle	(m^2)
R_c	radii of thermal contact circle	(m)	$P_{a,b}$	thermal power between particles	(W)

REFERENCES

[1] Brown, A.L., "Composite Fire Rubble Test Results: Implications for Models," Sandia Technical Report SAND2015-3494C, Sandia National Laboratories, The 7th FM Global Open Source CFD Fire Modeling Workshop, May 6-7, 2015, Four Points Conference Center, Norwood Ma, USA

[2] Brown, A.L., Jernigan, D., Dodd, A., "Intermediate-scale Fire Performance of Composite Panels under Varying Loads," Sandia Technical Report SAND2015-2369, Sandia National Laboratories

[3] Brown, A.L., Dodd, A., Erickson, K. L., "The Behavior of Carbon Fiber-Epoxy Based Aircraft Composite Materials in Unmitigated Fires," Sandia Technical Report SAND2012-0060 C, Sandia National Laboratories

[4] Engerer, J. D., Brown A.L., Christian, J. M., "Mass-Loss Measurements on Solid Materials after Pulsed Radiant Heating at High Heat Flux," Sandia Technical Report SAND2017-2145C, Sandia National Laboratories, 10th U.S. National Combustion Meeting organized by the Eastern States Section of the Combustion Institute, College Park, MA, April 23-26, 2017

[5] Brown, A.L., Dodd, A.B., Picket, B.M. "Enclosure Fire Tests for understanding Aircraft Composite Fire," Proceedings of the Sixth International Conference on Composites in Fire, CompositeLink Consultants (Limited), Newcastle upon Tyne, UK, 2011.

[6] Hubbard, J. A., Brown, A.L., Dodd, A.B., Gomez-Vasquez, S., and Ramirez, C.J., "Aircraft carbon fiber composite characterization in adverse thermal environments: radiant heat and piloted ignition flame spread," Sandia Technical Report SAND2011-2833.

[6] Hubbard, J. A., Brown, A.L., Dodd, A.B., Gomez-Vasquez, S., and Ramirez, C.J., "Aircraft carbon fiber composite characterization in adverse thermal environments: radiant heat and piloted ignition flame spread," Sandia Technical Report SAND2011-2833.

[7] Bagot, K., Hode, J. "Composite Material Fire Fighting Research," Presentation from the ARFF Working Group, FAA presentation, 8 October, 2010.

[8] Bai, Y.U., Keller, T., 2009a, "Modeling of Strength Degradation for Fiber-reinforced Polymer Composites in Fire," Journal of Composite Materials, 43 (21) pp. 2371-2385.

[9] Boyd, S.E.; Lesko, J.J.; Case, S.W., 2007, "Compression creep rupture behavior of a glass/vinyl ester composite laminate subject to fire loading conditions," Composites Science and Technology, 67 (15-16) pp 3187-3195.

[10] Brown, J. E., Braun, E., Twilley, W. H, "Cone Calorimeter Evaluation of the Flammability of Composite Materials," National Bureau of Standards, NBSIR 88-3733, March 1988.

[11] Burns, L.A., Feih, S., and Mouritz, A.P., 2010, "Compression Failure of Carbon Fiber-Epoxy Laminates in Fire," Journal of Aircraft, 47, 2, pp. 528-533.

[12] Delfa, G.L., J. Luinge, A. G. Gibson, "Next Generation Composite Aircraft Fuselage Materials under Post-crash Fire Conditions," Engineering Against Fracture: Proceedings of the 1st Conference, 2009, pp. 169-181.

[13] Elmughrabi, A.E., Robinson, M., Gibson, A.G., "Effect of stress on the fire reaction properties of polymer composite laminates," Polymer Degradation and Stability, 93, 1877-1883, 2008

[14] Fanucci, J.P., "Thermal Response of Radiantly Heated Kevlar and Graphite/Epoxy Composites," Journal of Composite Materials, Vol 21, 1987, p129-139.

[15] Kandare, E.; Kandola, B.K.; Myler, P.; Edwards, G.; 2010, "Thermo-mechanical Responses of Fiber-reinforced Epoxy Composites Exposed to High Temperature Environments. Part I: Experimental Data Acquisition," Journal of Composite Materials, 44, 26, pp. 3093-3114.

[16] La Delfa G.; Luinge, J.; Gibson, A. G.; 2009, "Next Generation Composite Aircraft Fuselage Materials under Post-crash Fire Conditions," Engineering Against Fracture, 169-181.

[17] Sorathia, U.; Beck, C.; Dapp, T.; 1993, "Residual Strength of Composites during and after Fire Exposure," Journal of Fire Sciences, 11, pp. 255-270

[18] Koo, H., Brown A.L., Voskuilen, T., Pierce, F., "Numerical study of pyrolysis and combustion of carbon fiber-epoxy composite," Sandia Technical Report SAND2017-2146C, Sandia National Laboratories, 10th U.S. National Combustion Meeting organized by the Eastern States Section of the Combustion Institute, College Park, MA, April 23-26, 2017

[19] Brown, A. L., "Multiphase Methods for Modeling Fire Environments," Sandia Technical Report SAND2016-10001C, Sandia National Laboratories, CCMT Multiphase Deep Dive, October 6-7, 2016, St. Petersburg, FL

[20] Koo, H., Brown A.L., Pierce, F., Voskuilen, T. “LES of a composite rubble fire,” Sandia Technical Report SAND2018-0810A, Sandia National Laboratories

[21] Kopacz, A. M., Bozinoski, R., Hewson, J. C., Dodd, A., Brown, A. L., Voskuilen, T. G., “Modeling Anisotropic Effects of carbon Fiber Reinforced Epoxy Composites in Fire Environments,” Sandia Technical Report SAND2016-6231 C, Sandia National Laboratories

[22] Koo, H., Hewson, J. C., Brown, A. L., “SIERRA/Fuego validation works for DNS, LES, and solid pyrolysis models,” Sandia Technical Report SAND2017-5120C, Sandia National Laboratories, The 9th FM Global Open Source CFD Fire Modeling Workshop, May 9, 2017, Four Points Conference Center, Norwood Ma, USA

[23] Brunini, V., Koo, H., Kopacz, A., Pierce, F., Subia, S., Voskuilen, T., “New capabilities in Aria and Fuego,” Sandia Technical Report SAND2016-12026C, Sandia National Laboratories

[24] Hewson, J. C., “Computational Predictions of Object Response in Propellant Fire Environments,” Sandia Technical Report SAND2017-3883PE, Sandia National Laboratories, Interagency Nuclear Safety Review Panel, April 2017

[25] Voskuilen, T. G., Pierce, F. G., Brown, A. L., Gelbard, F. E., Louie, D. L. Y., “Particle Resuspension Simulation Capability to Substantiate DOE-HDBK-3010 Data,” Sandia Technical Report SAND2016-9229C, Sandia National Laboratories

[26] Brown, A. L., Pierce, F., “Modeling Aerodynamic Break-up of Liquid Drops in a Gas Flow with Molecular Dynamics Analogy Methods,” Sandia Technical Report SAND2016-10465C, Sandia National Laboratories, Proceedings of the 2nd Thermal Fluid and Engineering Conference, TFESC-17710, April 2-5, 2017, Las Vegas, NV